Mon. Not. R. Astron. Soc. **279,** 171–179 (1996)

# Kinematics of ionized gas associated with the radio nucleus and lobes in the active galaxy IRAS 04210 + 0400

A. J. Holloway,[1] W. Steffen,[1] A. Pedlar,[2] D. J. Axon,[2★] J. E. Dyson,[1] J. Meaburn[1] and C. N. Tadhunter[3]

[1]*Department of Physics and Astronomy, University of Manchester, Schuster Laboratory, Oxford Road, Manchester M13 9PL*
[2]*Nuffield Radio Astronomy Laboratories, University of Manchester, Jodrell Bank, Macclesfield, Cheshire SK11 9DL*
[3]*Department of Physics, Hicks Building, University of Sheffield, Sheffield S3 7RH*

Accepted 1995 September 29. Received 1995 September 29; in original form 1995 July 25

## ABSTRACT

We have used high-resolution long-slit spectroscopy to investigate the ionized gas in the active galaxy IRAS 04210 + 0400 and its association with the radio structure.

We suggest that two of the ionized components are associated with the central double radio source, and observe that the relative positions of these components vary for different emission lines. Both results are consistent with the radio components representing the working surfaces of a pair of jets emerging from the centre of the galaxy. In this scenario, the optical emission in the centre arises behind the bowshocks produced by the jets in the interstellar medium.

The emission lines are detected and show a dramatic ($\approx 900$ km s$^{-1}$) spread in velocity at the position of the radio lobe hotspots. We suggest a model which explains this phenomenon as the result of a jet head emerging through the boundary between the interstellar and intergalactic media. A similar scenario has previously been suggested as a model to explain wide angle tail radio sources (WATs). Based on this model, we simulate the long-slit spectra of these regions and compare the results with the observations.

**Key words:** galaxies: active – galaxies: individual: IRAS 04210 + 0400 – galaxies: jets – galaxies: kinematics and dynamics – galaxies: Seyfert.

## 1 INTRODUCTION

Ionized gas has been known to be associated with active galactic nuclei (AGN), at least since Seyfert's discovery of broad lines from the bright star-like nuclei in several nearby spirals. There are at least two distinct nuclear components to this gas, consisting of the broad-line region (BLR) emitting permitted lines with velocity widths $\sim 3000$ km s$^{-1}$, and the narrow- (or forbidden-) line region (NLR) with linewidths of $\sim 500$ km s$^{-1}$. The BLR gas appears to be confined to a region less than a parsec in size at the centre of the galaxy (Rees, Netzer & Ferland 1989). The extent of the NLR is more difficult to quantify, but there is no doubt that in typical Seyferts the strongest NLR emission is confined to the central few hundred parsecs of the active galaxy. However, in the last decade high-sensitivity observations of active galaxies have revealed regions of ionized gas extending up to about 10 kpc (e.g. Markarian 6: Meaburn, Whitehead & Pedlar 1989).

There also are two distinct types of extended ionized regions. The extended narrow-line region (ENLR) is characterized by linewidths less than 100 km s$^{-1}$ and kinematics consistent with quiescent rotating gas in the host galaxy. It has been proposed that it consists of gas that is dynamically undisturbed by the central activity, although it is photoionized by the anisotropic UV emission from the AGN (Unger et al. 1987). This model, which has been reinforced by the detection of a number of 'wedge'-shaped ENLRs (e.g. NGC 1068: Pogge 1988; Unger et al. 1992; NGC 5252: Tadhunter & Tsvetanov 1989; Mrk 78: Pedlar et al. 1989), is consistent with photoionization by a cone of UV radiation from the nucleus.

The second type of extended ionized region (often loosely known as an EELR – extended emission-line region) also extends over approximately 10 kpc but exhibits linewidths of several hundred km s$^{-1}$ and shows velocities largely

★ESA Secondment, Space Telescope Science Institute, San Martin Drive, Baltimore, MD 21218, USA.

unrelated to the dynamics of the host galaxy. Often these regions are associated with radio jets (e.g. 3C 120: Axon et al. 1989; 3C 305: Heckman et al. 1982; Jackson et al. 1995) and are thought to represent the interaction of collimated ejection from the nucleus with the interstellar medium (ISM) or the intergalactic medium (IGM). In many cases, the gas appears to be photoionized by UV radiation from the nucleus, although it cannot be excluded that shock ionization is also important. The study of these EELRs provides information on the parameters of the host galaxy and its ISM and on those of the collimated ejection from the AGN. This information can be combined with the results from radio observations to constrain model calculations further. In this paper we report on a study of ionized gas associated with this latter type of extended emission-line region.

The galaxy IRAS 04210 + 0400 was first detected in scans of the *Infrared Astronomical Satellite* (*IRAS*) at 25 and 60 μm (Soifer et al. 1984). It has a redshift of $z = 0.0462$ (Beichman et al. 1985), implying a distance of 185 Mpc, at which 1 arcsec corresponds to 900 pc (assuming $H_0 = 75$ km s$^{-1}$ Mpc$^{-1}$). Further work by Beichman et al. (1985) identified the *IRAS* source with a spiral galaxy having an integrated *R*-band magnitude of 16.3. Their spectroscopy revealed a Seyfert type 2 emission-line nucleus, although its association with extended radio emission was unusual. Hill et al. (1988) showed the radio structure to consist of a central double source and large-scale ($\sim$25 kpc) double radio lobes extending beyond the optical galaxy. Typically, the nuclei of spiral galaxies, including Seyferts, are radio-quiet objects, with radio luminosities of $\sim 10^{20-21}$ W Hz$^{-1}$ at 20-cm wavelength. If radio emission is observed, the structures are usually smaller than 600 pc (e.g. Ulvestad & Wilson 1984). Although radio 'lobes' are not unknown in spiral galaxies (e.g. NGC 3079 and 5548), IRAS 04210 + 0400 would be a rare example of a spiral galaxy with associated radio structure more like that of a Fanaroff–Riley I (FRI) radio galaxy with hotspots and diffuse lobes. However, Hill et al. (1988) have questioned the classification of IRAS 04210 + 0400 as a spiral, and suggested that the 'spiral arms' may be associated with the radio ejecta. The observed 20-cm radio luminosity of $2.4 \times 10^{23}$ W Hz$^{-1}$, the large radio lobes, and the narrow emission-line spectrum more nearly fit the definition of a narrow-line radio galaxy (NLRG) which is associated with elliptical galaxies.

The radio galaxies 3C 305 (Heckman et al. 1982; Jackson et al. 1995), 4C 29.30 (van Breugel et al. 1986) and 4C 26.42 (van Breugel, Heckman & Miley 1984) have similar radio and optical properties. They all show radio jets which, starting from hotspots, flare and bend into extended radio lobes. Nevertheless, IRAS 04210 + 0400 is distinguished from these cases through the alignment of the bent lobes with the spiral structure and the high symmetry of its radio and optical emission.

In this paper we concentrate on the kinematics and spatial positions of the spectral features. In Section 2 we present the imaging and spectral observations obtained at the William Herschel Telescope (WHT) and at the Isaac Newton Telescope (INT) on La Palma, respectively. In Section 3 we discuss the observational results and outline a model which reproduces the main spectral features. Our conclusions are summarized in Section 4.

## 2 OBSERVATIONS AND RESULTS

### 2.1 WHT imaging

An *R*-band image, with 800-s exposure, of the galaxy was obtained using the 4.1-m William Herschel Telescope on 1993 December 13. An EEV CCD was used at the auxiliary focus with the 22 μm square pixels providing an image scale of 0.1 arcsec pixel$^{-1}$. The image was processed in the usual manner but not flat-fielded. This is not a serious problem, however, as the area of interest is small and the image was not to be used for photometry. The seeing during the observation was typically 1.6 arcsec and the images were also blurred by a slight shift in focus of the telescope during the exposure.

The image is shown in Fig. 1 (opposite p. 172) with the radio map contours and slit position overlaid. It is displayed on a logarithmic intensity scale to enable the bright core and faint spiral features to be seen.

### 2.2 INT spectroscopy

Long-slit spectra were obtained using the Intermediate Dispersion Spectrograph (IDS) and GEC7 CCD at the Cassegrain focus of the 2.5-m Isaac Newton Telescope on La Palma over the nights of 1993 December 4 and 6. The 500-mm camera was used to provide a spatial scale of 0.3 arcsec pixel$^{-1}$ and a wavelength dispersion of 0.48 Å pixel$^{-1}$ over the 590 × 400 pixel array. The two exposures were taken at position angle 0° centred on the nucleus to coincide with the radio axis. Observing conditions varied for the exposures: the [O III] 5007-Å region centred on 5160 Å was observed for 3600 s under 1.6-arcsec seeing and the Hα region centred on 6950 Å was observed for 6000 s with 1.0-arcsec seeing and a 0.7-arcsec slit width. The wavelength resolution, as determined from the arc spectra, was 1.1 Å (63 km s$^{-1}$ at [O III] 5007 Å and 48 km s$^{-1}$ at Hα).

The data were processed at the University of Manchester node of the UK Starlink network using programs from the FIGARO, TWODSPEC and KAPPA packages. The bias level of the CCD was measured from the overscan region of the chip and a mean value subtracted. The spectra were calibrated in wavelength and corrected for curvature along the slit length using the copper–neon arc lamp spectrum. When wavelength-calibrated, the background sky lines were removed by averaging two strips which were clear of object data on either side of the continuum and subtracting this sky spectrum from each row. The spectra were corrected for the instrumental response and flux-calibrated using the standard star HD 93521.

Position–velocity maps of the [O III] 5007-Å and Hα + [N II] lines are presented in Figs 2(a) and (b). They are displayed with a logarithmic intensity scaling to enable both bright and faint features to be seen clearly. The [O III] 5007-Å line is broad ($\sim$400 km s$^{-1}$) close to the nucleus, and the more extended gas has linewidths of $\sim$800 km s$^{-1}$. The Hα + [N II] 6548, 6584-Å plot shows similar velocities to the [O III] 5007-Å, but of particular note are the large linewidths (900 km s$^{-1}$) seen in Hα approximately 7 arcsec to the south of the nucleus. In the nucleus we can detect a number of fainter lines in spectra produced by co-adding data over the central 1 arcsec. Hβ, [O III] 4959-Å and [O III] 5007-Å lines are visible in Fig. 3(a), and [N II] 6548-Å, Hα,

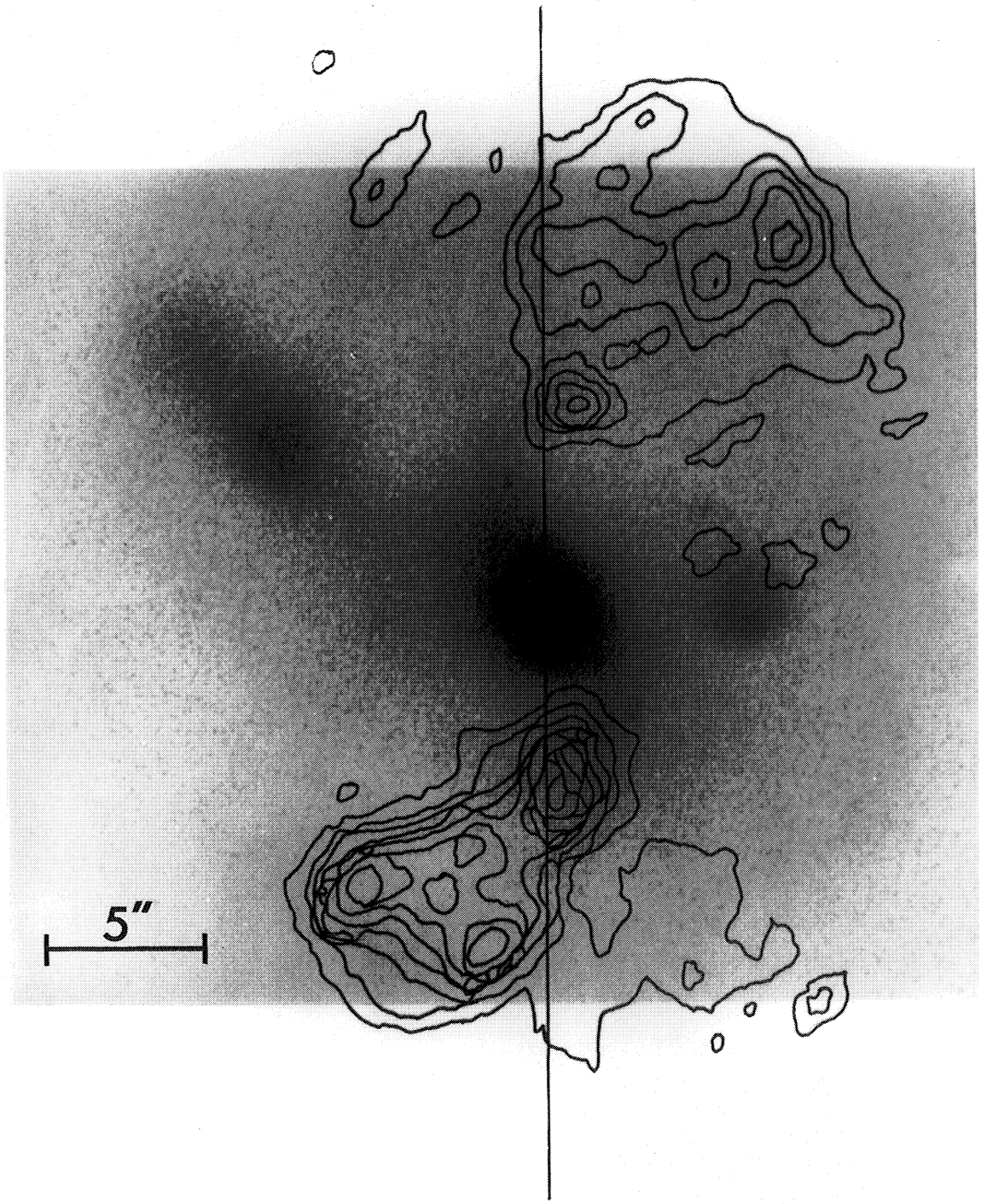


**Figure 1.** WHT *R*-band image displayed with logarithmic scaling and VLA 6-cm radio contours (Hill et al. 1988) superimposed.

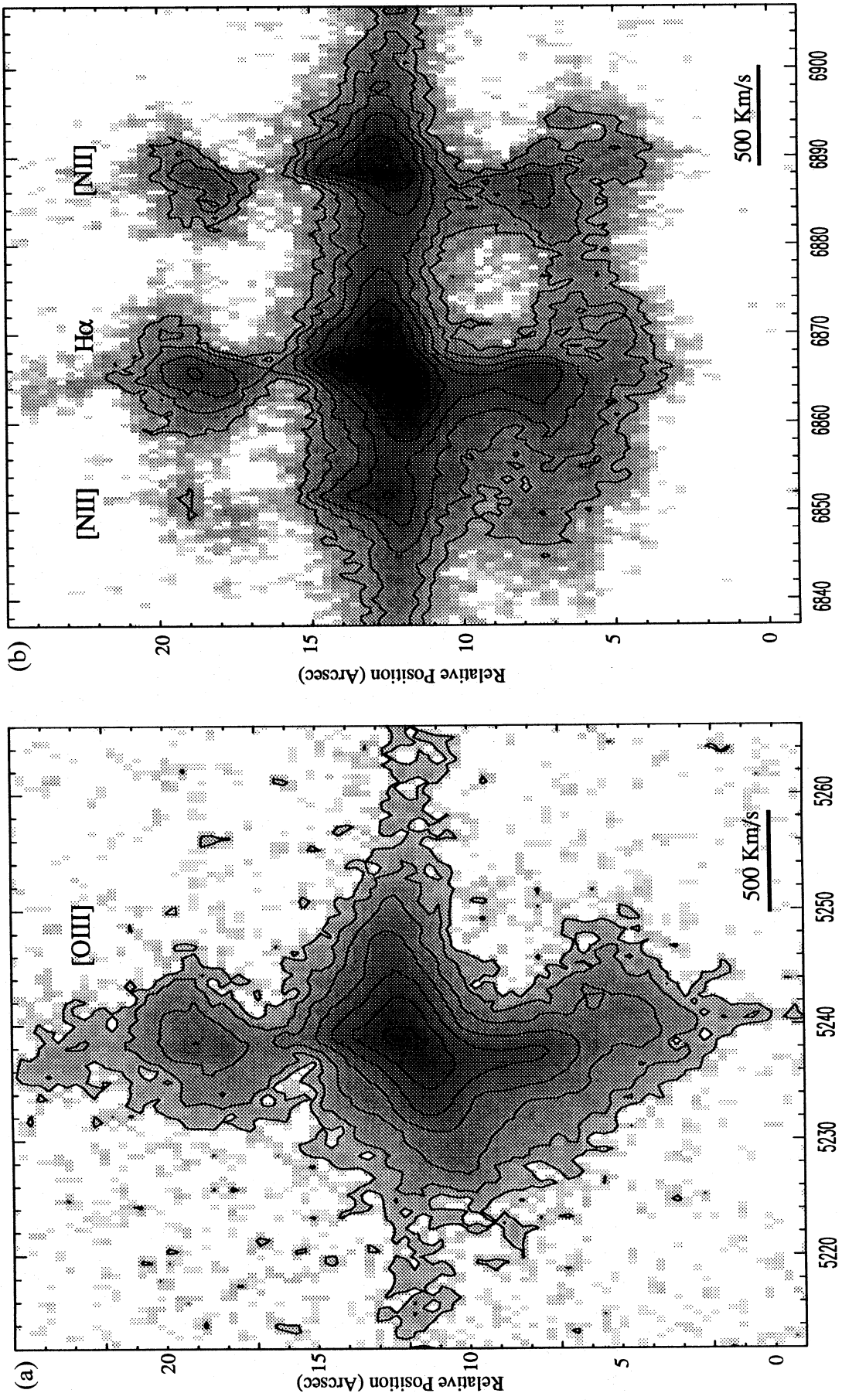


**Figure 2.** INT IDS long-slit spectra, displayed on a logarithmic scaling, for the wavelength regions containing (a) the [O III] 5007-Å line with contours at 1, 2, 5, 10, 20, 40 and 80 per cent of the peak intensity, and (b) Hα + [N II] 6548, 6584-Å lines with contours at 1, 2, 5, 10, 20, 40, 70 and 90 per cent of the peak intensity.

[N II] 6584-Å and [S II] 6716, 6731-Å lines are visible in Fig 3(b).

## 3 DISCUSSION

In this section we discuss the observations, focusing on the classification of the galaxy from broad-band imaging (Section 3.1), and the peculiar gas kinematics observed in the core (Section 3.2) and in the regions around 5 arcsec north and south of the core (Section 3.3). In Section 3.4 we outline a simple model which reproduces the peculiar extended features found in the long-slit emission-line profiles.

### 3.1 The classification of IRAS 04210 + 0400

In our *R*-band image (Fig. 1), we have detected emission from IRAS 04210 + 0400 out to distances of 8.5 and 9.5 arcsec north and south of the nucleus, respectively. This gives a projected diameter for the galaxy of 16 kpc. The central bulge-like region has a radius of ~2 arcsec (1.8 kpc) and the spiral features extend a further ~7 arcsec (6.3 kpc). To the north-east of IRAS 04210 + 0400 lies a possible companion galaxy, this association being suggested by its redshift of $z = 0.047$ (Hill et al. 1988) which is similar to that of IRAS 04210 + 0400. The most luminous part of this companion is located 11 arcsec (10 kpc) from the centre of the galaxy and the faint extended emission extends over 7 arcsec (6.3 kpc) diametrically away from IRAS 04210 + 0400. At 6.5 arcsec (5.9 kpc) west of IRAS 04210 + 0400 there is a faint object which may also be interacting with the galaxy, and further spectroscopy will be required to check that it is not simply an object along our line of sight.

The spiral features originate from the central region at position angle ~30° and appear to terminate at position angle ~0°, in the vicinity of the 6-cm VLA radio lobe hotspots north and south of the nucleus. The radio lobes appear to continue the curve defined by the arms out to distances of 17 arcsec (15.3 kpc) and 14 arcsec (12.6 kpc) north and south, respectively. If the curve defined by the arms is continued to the limit of the radio emission, the position angle of this point is ~ −30°.

If the galaxy is a spiral, then the position of the spiral arms with respect to the radio lobes is a coincidence and the extended rotation pattern of the lobes is then explicable as a product of the galactic rotation, assuming the jet to be near the disc of the galaxy. Pressure bending as the jet leaves the galactic environment could also lead to the bending of the radio lobe, although then the observations that both optical and radio features follow a similar curve would be a coincidence.

If, on the other hand, the galaxy is an elliptical, then a different mechanism to produce the spiral features is required. Such a model was suggested by Hill et al. (1988), in which the spiral features are the photoionized remnants of the radio jet. The clear alignment between the nuclear double and the hotspots of the extended lobes would suggest that the radio jet moves along this line and not in a curved path along the spiral features. Material swept up by the passage of the jet would then have been photoionized by the central UV source and would since have moved by rotational motions. This explains the alignment of the spiral photoionized jet remnant and the radio lobes, and provides an argument against the idea of the extended features being tidal tails.

The exact nature of the spiral features could be decided by further spectroscopy of the region. As a working hypothesis, in the following discussion we take the observed galaxy to be an elliptical, with photoionized jet remnants.

### 3.2 The nucleus

The integrated spectrum of the nuclear region (Fig. 3) shows FWHM linewidths for the [O III] 5007-Å, Hα and

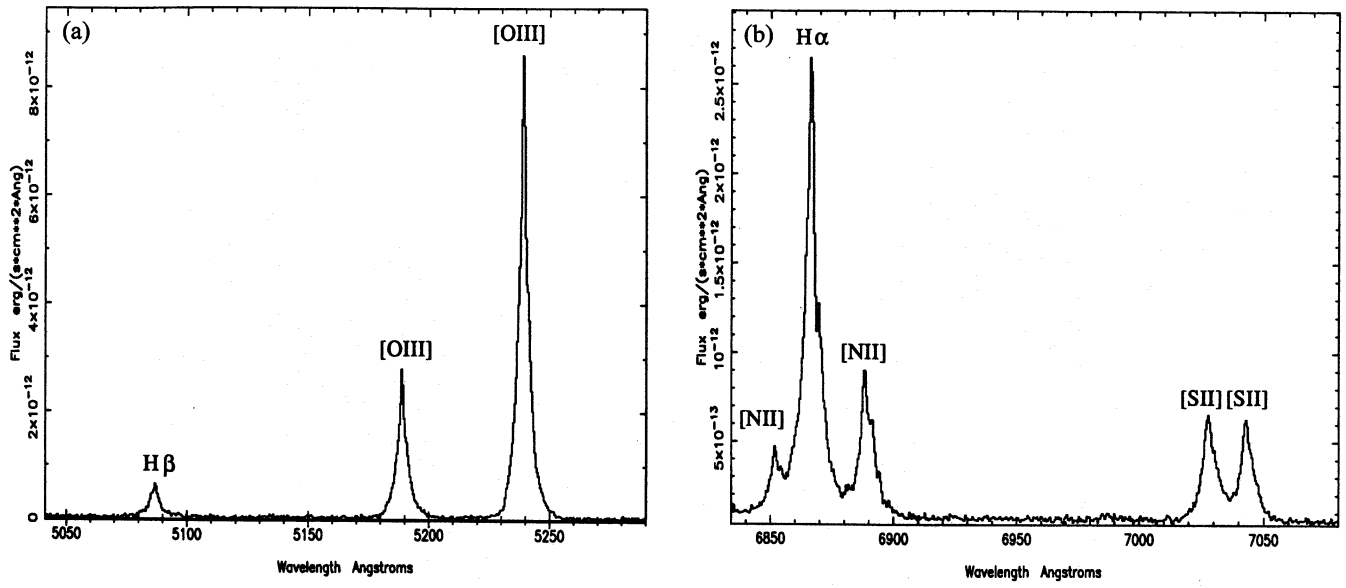


**Figure 3.** INT IDS spectra of the nucleus of IRAS 04210 + 0400 over the wavelength ranges (a) 5040–5290 Å and (b) 6835–7080 Å.

[S II] lines of 400, 300 and 330 km $s^{-1}$ respectively. These are typical for the NLRs of Seyfert 2 and narrow-line radio galaxies. We see no evidence of broader permitted lines (representative of a BLR).

In our long-slit spectra, asymmetric spatial structure is found in the core region (Fig. 2). We identify several separate components in velocity and space. Their positions, relative to the peak of the continuum, are shown in Table 1.

The brightest peak of [O III] 5007-Å emission lies 0.51 arcsec to the north of the continuum. The broad blue- and redshifted components are located 0.47 arcsec south and 0.78 arcsec north of the continuum peak, respectively. The intensity peaks of Hα, [N II] and [S II] are found to be closer to the galaxy core than those of the corresponding [O III] 5007-Å components. Although the seeing for the [O III] 5007-Å observation (1.6 arcsec) was considerably poorer than that for the others (1 arcsec), we exclude this as a possible explanation of the difference as the components are well separated in velocity space and do not contaminate each other.

We find systematic shifts between peak positions of the different lines. The order of appearance of peaks is the same for the northern and the southern components, except for [N II]. Separations to the south are smaller than to the north.

**Table 1.** Separations of central components in different spectral lines, relative to the continuum position (±0.02 arcsec). For comparison, the separation between the central radio components is 0.71 arcsec. Positive separations are to the north.

| Region | Red comp. | Peak comp. | Blue comp. |
|---|---|---|---|
| [O III] 5007Å | 0.78±0.05″ | 0.51±0.05″ | -0.47±0.05″ |
| Hα | 0.41±0.03″ | 0.37±0.03″ | -0.27±0.03″ |
| [N II] 6584Å | 0.50±0.03″ | 0.29±0.05″ | -0.11±0.05″ |
| [S II] 6716Å | 0.45±0.05″ | 0.34±0.06″ | -0.14±0.03″ |

In Figs 4 and 5 we show cuts through the core sections of the [O III] 5007-Å long-slit spectra in the spatial direction, showing the intensity along position angle 0°. In these plots the relative strengths of the cuts are arbitrary and only the spatial information is used. We include a two-component Gaussian fit to radio data obtained from a 6-cm VLA map which shows a compact double source, oriented along position angle 0° with a separation of 0.71 arcsec (resolution 0.55 arcsec: Hill et al. 1988). The position of the radio with respect to the optical data is not exactly known, so we have adjusted the position to be symmetric with respect to the broad blue- and redshifted components, following our suggestion that they are related to each other.

The association of radio and [O III] 5007-Å emission in the NLRs of Seyferts has been established in a number of cases (e.g. NGC 5929: White et al. 1986; Mrk 78: Pedlar et al. 1989). Models have been developed to account for the association in which the radio plasma interacts with the ISM in the bowshocks of expanding plasmons or working surfaces of jets (Pedlar, Unger & Dyson 1985; Wilson & Ulvestad 1987; Taylor, Dyson & Axon 1991). Based on our observations, we suggest that this scenario also applies to the central region of IRAS 04210 + 0400.

However, the separation between the locations of the [O III] 5007-Å and Hα regions when comparing the red and blue components is ~0.3 arcsec (300 pc). If these components are produced by the suggested bowshocks, photoionization is not able to explain the large difference in position of these spectral lines, taking into account the high particle density of ~$10^4$ $cm^{-3}$ (from the [S II] 6716, 6731-Å ratio) and the inferred bowshock velocity of ~300 km $s^{-1}$. Instead we suggest that the gas is mainly collisionally ionized, which is consistent with the strength of the [S II] 6716, 6731-Å lines. In this view, the difference in position of the [O III] 5007-Å and Hα regions arises from the decrease in shock speed normal to the bowshock surface at larger distances from the apex. According to Cox & Raymond (1985), the [O III] 5007-Å emission dominates over the Hα emission

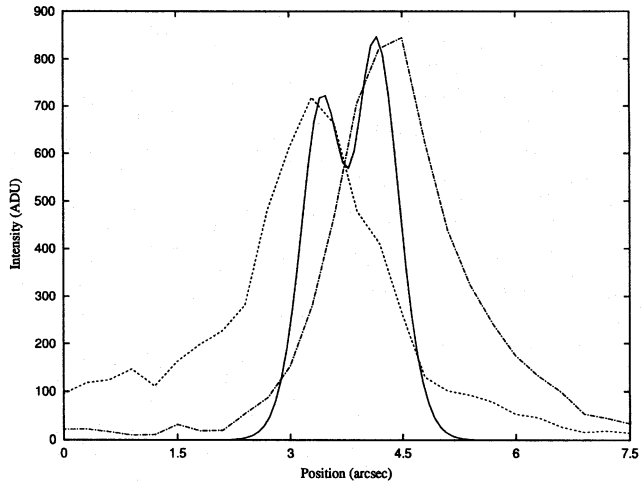


**Figure 4.** Plot of a two-component Gaussian fit to the central radio intensity profile (Hill et al. 1988, solid line) and cuts through blue (dotted) and red (dot–dashed) components from the [O III] 5007-Å emission. The wavelength range of the cuts is 5232–5236 Å for the blue and 5245–5248 Å for the red component (see Fig. 2a).

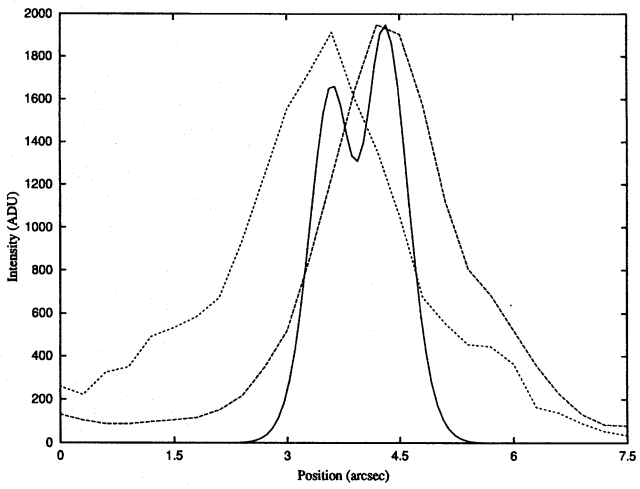


**Figure 5.** Plot of a two-component Gaussian fit to the central radio intensity profile (Hill et al. 1988, solid line) and cuts through the normalized continuum (dotted) and the peak intensity (dashed) components from the [O III] 5007-Å emission. The wavelength range of the cuts is 5105–5167 Å for the continuum and 5238–5240 Å for the peak component (see Fig. 2b).

at shock speeds higher than $\sim 100$ km s$^{-1}$, while the reverse is true for lower shock speeds. In our case the H$\alpha$ emission would come from positions on the bowshock where the normal to the surface makes angles of $\geq 70°$ with the direction of propagation of the apex.

This interpretation does not account for the peak spectral component located 0.5 arcsec (for [O III] 5007 Å) north of the continuum (Fig. 5). Within the error, this separation is identical to the separation between the radio components. Therefore we cannot exclude the possibility that this strong feature is associated with the northern radio component. In this case the southern radio component could represent the core of the galaxy and be associated with the continuum emission.

At present there is no spectral index information on the nuclear double, and hence one of the radio components could be a compact flat-spectrum core which would be associated with the optical continuum nucleus. Radio observations at two different frequencies will be carried out to determine whether this is the case. However, the high overall structural and spectral symmetry in IRAS 04210 + 0400 (analogous to NGC 5929 and other Seyferts, in which flat-spectrum cores are rare) leads us to adopt the working hypothesis that the two radio components are associated with the heads of a two-sided jet.

### 3.3 Extended emission-line regions

An important result of our observations is the spatial and spectral resolution of ionized gas with high velocity extending north and south more than 10 kpc from the nucleus (Figs 1 and 2). The basic structure can be appreciated best in the [N II] 6584-Å line (Fig. 2b). The northern hotspot at around 5-arcsec separation from the centre shows a clearly 'V'-shaped structure, where the redshifted arm is stronger and more extended. In H$\alpha$ and [O III] 5007 Å a corresponding structure is found, although the blueshifted arm is less obvious.

The southern hotspot (at approximately the same core separation) shows a very similar, but inverted, structure, although even better defined: most of the emission spreads into a blue wing, with increasing negative relative velocity with a larger separation from the core. At a lower brightness level, emission is seen spreading into a red wing. Although the structure is marginally resolved, the observation is suggestive of two components of acceleration or possibly a ring-like structure in the velocity-space map. We find a considerable difference in the [O III] 5007-Å line (Fig. 2a), in that the inverted 'V'-shape to the south is not obvious and instead all or most of the emission seems to be in the redshifted wing.

There are three simple possible kinematic interpretations of such 'V'-shaped structures in the velocity map. They may arise from real acceleration of the gas. Alternatively, the gas may have a certain high velocity when the line emission starts and the direction of the velocity vector may just change. Naturally, the third possibility is a combination of both effects.

### 3.4 Modelling the spectra of the hotspots

Jets in radio galaxies of moderate luminosities ($< 10^{25}$ W Hz$^{-1}$) can flare in only a few jet diameters and show very large opening angles of up to 90° into diffuse lobes or tails (O'Donoghue, Eilek & Owen 1993). These structures often bend very near the transition point, as is the case for IRAS 04210 + 0400 (see Fig. 1). Norman, Burns & Sulkanen (1988) and Loken et al. (1995) have modelled this phenomenon to explain the structure of wide angle tail radio galaxies (WATs) in terms of an initially moderately supersonic jet (Mach number 2–5) passing through a shock or contact discontinuity in the ambient gas where the jet flow becomes subsonic. The jet is then disrupted and entrains external gas, which becomes turbulent, and large- and small-scale eddies then develop. Such a shock in the ambient medium could be due to a supersonic galactic wind moving into the surrounding intergalactic medium.

We suggest that a similar scenario applies to IRAS 04210 + 0400 at the position of the radio hotspots. A supersonic jet propagates through the interstellar medium and passes through a transition region at the edge of the galaxy (see Fig. 6). It emerges from the main galaxy at the position of the hotspots. Here it goes subsonic, disrupts and expands with a large opening angle, producing the bent conical lobes. Ambient gas is entrained and accelerated to several hundred kilometres per second, thereby radiating in the observed emission lines. In the case of IRAS 04210 + 0400 this region is about 2.5 arcsec (2.3 kpc) in size, starting at 4.5-arcsec (4 kpc) separation from the core. This is the extension of both the enhanced optical and strongest radio emission.

It is worth noting that Owen, O'Dea & Keel (1990) conducted a search for optical line emission from these flaring regions in WAT sources but found no significant emission from the five objects that they studied.

We model the long-slit emission-line spectra using a simple parametrized description of the emission and velocity field of the ionized gas flow. Fig. 6 shows a schematic view of our model, of which we will give an outline here. A full account of the theoretical model will be given in a forthcoming paper (Steffen et al., in preparation).

We concentrate on the kinematics of the hotspot positions, and model the emission-line source as a collimated outflow which flares when passing through the boundary between the ISM and the IGM (see Fig. 6). The outflow opens gradually to an effective half-opening angle of $\sim 45°$ (where the exponentially decaying emissivity becomes negligible). The long-slit line profile is most dependent on the orientation of the outflow with respect to the observer's line of sight and the orientation of the spectrometer slit. The detailed shape of the outflow and the change in emissivity as a function of distance from the starting point influence only the detail of the simulated spectrum and not the gross features.

The velocity is assumed to be constant (600 km s$^{-1}$ in the southern and 350 km s$^{-1}$ in the northern outflow), such that the structure found in the long-slit spectra results from the change in flow direction of the gas. For simplicity, we assume the flow to be concentrated in a sheet of Gaussian transverse emissivity distribution, as shown schematically in Fig. 6.

In Fig. 7 we compare the observed H$\alpha$ and [N II] line complex with our model. The axes of the outflows are inclined to the sky plane at angles of 15° (north) and 20°

(south), both towards the observer such that the directions of propagation are not exactly collinear. This is suggested by the slight blueshift of both hotspots with respect to the central region. The slit direction is north–south and the axes of the outflows are oriented at position angles $-25°$ (north) and 150° (south) with respect to the slit direction (north–south), consistent with the observed directions of the radio lobes. The slit is sufficiently broad to collect all the emission from the outflows.

The simulations reproduce the basic features of the observed spectral line structure of the hotspot regions. Thus the optical observation and modelling of the interaction of jets with the transition region between the ISM and the IGM could be an important tool to study several aspects of the galaxy environment. In particular, they provide information about the velocities in the extragalactic jets, which are subject to debate. Otherwise, such direct kinematic information is not available on kiloparsec scales.

## 4 CONCLUSIONS

We have measured the spatial and velocity structure of the emission features in the nucleus and coincident with the radio hotspots in the lobes of IRAS 04210 + 0400.

(i) We have observed a Seyfert type 2 spectrum for the nucleus of IRAS 04210 + 0400 and, with the evidence for it being an elliptical galaxy, suggest that we are looking at a narrow-line radio galaxy, albeit with apparent spiral photoionized jet remnants.

(ii) In the nucleus we can identify broad velocity components with a similar spatial separation to the double radio source. This suggests that we are looking at a two-sided jet with emission associated with the radio jets. The observations can be explained by a bowshock model with collisional excitation.

(iii) We see extended emission features with high velocity dispersion at the position of the radio hotspots in the lobes. This is consistent with a jet undergoing expansion in the IGM. We have modelled this expansion as a jet which passes through the ISM/IGM boundary. Our expanding outflow model reproduces the observed long-slit spectra in these regions.

(iv) This object provides a unique opportunity to study the interaction of a jet with an ISM/IGM boundary at both optical and radio wavelengths. This gives kinematic and morphological information that so far has not been obtained for WAT sources which show a similar phenomenology in the radio (although on a larger scale than here).

## ACKNOWLEDGMENTS

AJH and WS acknowledge the receipt of a PPARC studentship and a PPARC research associateship respectively. Thanks are due to the support staff of the INT and WHT

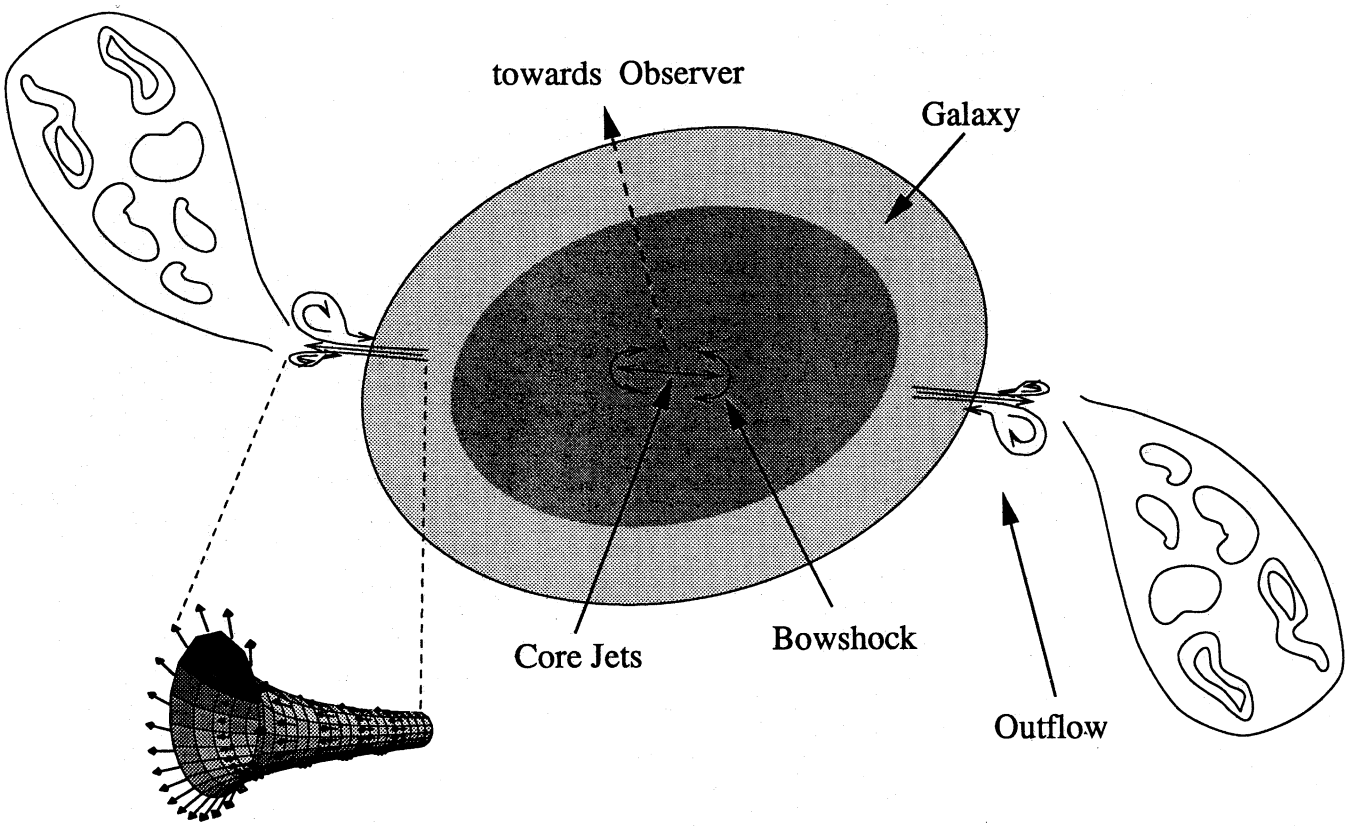


**Figure 6.** A schematic view of a model for IRAS 04210 + 0400 with a central double bowshock and an expanding outflow for the emergent jets at the galaxy/IGM boundary.

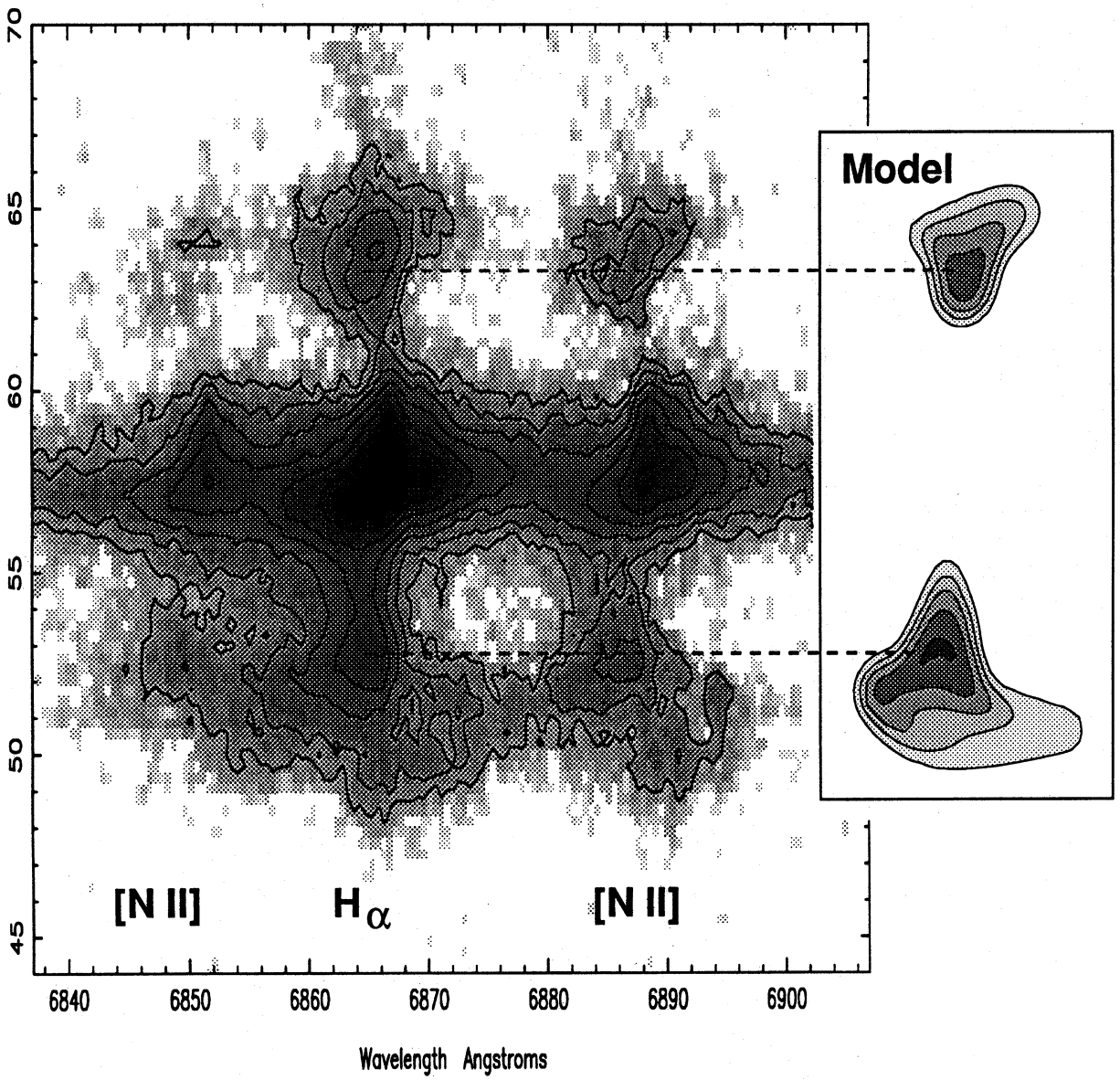


**Figure 7.** A comparison between the observed spectra and the spectrum generated by the outflow model for the emerging jets.

during our observing runs. We thank R. J. R. Williams and A. Wilkinson for useful discussions.

## REFERENCES

Axon D. J., Pedlar A., Unger S. W., Meurs E. J. A., Whittle D. M., 1989, Nat, 341, 631
Beichman C. et al., 1985, ApJ, 293, 148
Cox D. P., Raymond J. C., 1985, ApJ, 298, 657
Heckman T. M., Miley G. K., Balick B., van Breugel W. J. M., Butcher H. R., 1982, ApJ, 262, 529
Hill G. J., Wynn-Williams C. G., Becklin E. E., MacKenty J. W., 1988, ApJ, 335, 93
Jackson N., Sparks W. B., Miley G. K., Macchetto F., 1995, A&A, 296, 339
Loken C., Roettiger K., Burns J. O., Norman M., 1995, ApJ, 445, 80
Meaburn J., Whitehead M. J., Pedlar A., 1989, MNRAS, 241, 1
Norman M. L., Burns J. O., Sulkanen M. E., 1988, Nat, 335, 146
O'Donoghue A. A., Eilek J. A., Owen F. N., 1993, ApJ, 408, 428
Owen F. N., O'Dea C. P., Keel W. C., 1990, ApJ, 352, 44
Pedlar A., Unger S. W., Dyson J. E., 1985, MNRAS, 214, 463
Pedlar A., Axon D. J., Meaburn J., Unger S. W., Whittle D. M., 1989, MNRAS, 238, 863
Pogge R. W., 1988, ApJ, 328, 519
Rees M. J., Netzer H., Ferland G. J., 1989, ApJ, 347, 640
Soifer B. T. et al., 1984, ApJ, 278, L71
Tadhunter C., Tsvetanov Z., 1989, Nat, 341, 422
Taylor D., Dyson J. E., Axon D. J., 1992, MNRAS, 255, 351
Ulvestad J. S., Wilson A. S., 1984, ApJ, 285, 439
Unger S. W., Pedlar A., Axon D. J., Whittle M., Meurs E. J. A.,

1987, MNRAS, 228, 671
Unger S. W., Lewis J. R., Pedlar A., Axon D. J., 1992, MNRAS, 258, 371
van Breugel W. J. M., Heckman T. M., Miley G. K., 1984, ApJ, 276, 79
van Breugel W. J. M., Heckman T. M., Miley G. K., Filippenko A. V., 1986, ApJ, 311, 58
Whittle M., Haniff C., Ward M., Meurs E., Pedlar A., Unger S. W., Axon D. J., Harrison B., 1986, MNRAS, 222, 189
Wilson A. S., Ulvestad J. S., 1987, ApJ, 319, 105